Ceramics International 43 (2017) 5708–5714

Contents lists available at ScienceDirect

Ceramics International

journal homepage: www.elsevier.com/locate/ceramint

Comparison of corrosion behavior of Ti_3SiC_2 and Ti_3AlC_2 in NaCl solutions with Ti

M. Zhu[a], R. Wang[b], C. Chen[b], H.B. Zhang[b,*], G.J. Zhang[c]

[a] College of Materials Science and Engineering, Xi'an University of Science and Technology, Xi'an 710054, China
[b] Innovation Research Team for Advanced Ceramics, Institute of Nuclear Physics and Chemistry, China Academy of Engineering Physics, Mianyang 621900, China
[c] State Key Laboratory for Modification of Chemical Fibers and Polymer Materials, Research Institute of Functional Materials, Donghua University, Shanghai 201620, China

ARTICLE INFO

Keywords:
Passivation behavior
Corrosion mechanism
MAX phase
NaCl solution

ABSTRACT

Corrosion behavior of self-sintered, ternary-layered titanium silicon carbide (Ti_3SiC_2) and titanium aluminum carbide (Ti_3AlC_2) fabricated by an in-situ solid-liquid reaction/hot pressing process was investigated by potentiodynamic polarization, potentiostatic polarization and electrochemical impedance spectroscopy in a 3.5% NaCl solution. Commercially pure titanium (Ti) was selected for comparison through XRD, XPS, SEM and EDS examinations for elucidating both the passivation behavior and corrosion mechanism of the alloys. Both Ti_3SiC_2 and Ti_3AlC_2 exhibited significantly superior passivation characteristics compared to Ti; Ti_3SiC_2 also showed better corrosion resistance. The silicon/aluminum site is prone to attack, and the difference in the diffusion rate between the A-site atoms and titanium decreases the passivation ability of the MAX phase. CP titanium exhibited a lower passivation current density and did not undergo breakdown in the test potential region while two MAX phases are destroyed. Nevertheless, the corrosion resistances of Ti_3SiC_2 and Ti_3AlC_2 are comparable to that of CP titanium.

1. Introduction

Interesting combination of metallic and ceramic properties in a class of ternary-layered ceramics known as the $M_{n+1}AX_n$ (n=1,2,3) phases—wherein M is a metal selected from group IIIB, IVB, VB, VIB or VIII; A is selected from group IIIA, IVA, VA or VIA and/or a mixture thereof; and X is carbon and/or nitrogen has received considerable attention lately [1]. A significant number of papers on structural [2], thermal [3], electrical [2,4,5], and mechanical [6] properties of MAX phases have been published. MAX phases exhibit high damage tolerance, high chemical stability, low density, and excellent corrosion resistance, typical of ceramics as well as electrical and thermal conductivity, machinability, thermal shock resistance, and ductility at high temperature, typical of metals.

Their unique properties make MAX phases attractive prospective materials for applications in metallurgical or energy related systems, chemical and/or electrochemical engineering, and even sewage treatment. Few studies have focused on electrochemical behavior of these phases [7–12]. Barsoum and co-workers have conducted a series of studies on the electrochemical corrosion behaviors of selected MAX phases (Ti_3SiC_2, Ti_3AlC_2, Ti_3CeC_2 Ti_2AlC, V_2AlC, etc.) in contact with strong acid and/or strong base solutions such as HCl, H_2SO_4, or NaOH [10]. They attributed the exceptional corrosion resistance of Ti_3SiC_2 superior to the corrosion resistance of pure Ti the formation of a thin SiO_2-based passivation layer [9]. The passivation film formed on Ti_3AlC_2 [10,12] contained Ti, which made its corrosion resistance inferior to that of Ti_3SiC_2. Zhang et al. [13–16] investigated the hydrothermal oxidation behaviors of Ti_3SiC_2 and Ti_3AlC_2, followed by corrosion behavior of selected MAX phases in hot concentrated HCl solution. It was demonstrated that the corrosion resistance was closely related to the nano-laminated crystal structure as well as the differences between the A and M-X layers of MAX phases. A-sites Al atoms were more prone to attack than Si atoms in the same layer, which resulted in the survival of Ti_3SiC_2 and disintegration of Ti_3AlC_2 in hot HCl solutions [17]. These results indicated that the passivation and corrosion mechanisms may be different from those of pure metals such as Ti in this case. However, the corrosion mechanisms have not been extensively studied and differences in the passivation processes of MAX phases and vale metals are still unknown.

Corrosion resistance of MAX phases in either aqueous acid or base may be attributed to formation of passivation layers. It has been suggested that some MAX phases may potentially be used as anode

---

[*] Corresponding author.
E-mail address: hbzhang@caep.cn (H.B. Zhang).

http://dx.doi.org/10.1016/j.ceramint.2017.01.111
Received 25 November 2016; Received in revised form 11 January 2017; Accepted 22 January 2017

and/or cathode by the chlor-alkali electrolysis industry [11], as it is often suggested they may be resistant to corrosion in relatively mild corrosive environments. However, this is perhaps not always true in an ocean environment. Understanding what happens during passivation and corrosion in NaCl solution will help clarifying the corrosion mechanisms of MAX phases and is important for their application in NaCl containing environments.

Ti_3SiC_2 and Ti_3AlC_2 are the most popular MAX phases and are the most widely studied in the group. The motivation for this work is to further understanding of the corrosion and passivation mechanisms of these materials in NaCl and to clarify their differences with passivation and corrosion mechanisms of commercially pure Ti.

2. Experimental

2.1. Sample preparation

Polycrystalline bulk Ti_3SiC_2 and Ti_3AlC_2 materials were synthesized by in-situ solid-liquid reaction/hot pressing process. Ti_3SiC_2 was hot pressed and sintered in a graphite die using mixed TiC, Ti and Si powders in a ratio of 2:1:1.1. Samples were heated to 1400 ℃ and held for 120 min at 40 MPa. Ti_3AlC_2 was fabricated in the same manner from TiC, Ti and Al powders with a ratio of 2:1:1.2 at 1500 ℃ and 40 MPa for 120 min. Test coupons measuring 10 mm×10 mm×3 mm in size were cut from the as-prepared bulk Ti_3SiC_2 and Ti_3AlC_2 samples using an electrical discharge machining method (EDM) and subsequently sealed with epoxy after connecting to a copper wire to form a working electrode. To obtain reproducible surfaces, test surfaces were wet-ground successively with SiC emery papers to 2000 grit and then ultrasonically cleaned with acetone followed by rinsing with distilled water before drying. Commercially pure Ti, chosen for comparative study of the corrosion and passivation behaviors, was also sealed in epoxy, except for the test surface, which was wet-ground to 2000 grit, ultrasonically cleaned in acetone and rinsed with distilled water before drying.

2.2. Electrochemical measurements

Electrochemical tests were performed on a Zahner Zennuim potentiostat/galvanostat (ZAHNER-elektrlk GmbH & Co. KG, Germany) controlled by Thales Z2.22 software connected to a conventional three-electrode electrochemical cell filled with a 3.5% NaCl solution at room temperature. A Pt foil counter electrode and Ag/AgCl reference electrode (0.197 V vs. standard H electrode, SHE), were placed in their appropriate positions. Potentiodynamic polarization measurements were carried out from −300 mV vs. OCP to breakdown with a scan rate of 0.333 mA/s. The EIS (electrochemical impendence spectroscopy) curves obtained after immersion and potentiostatic polarization at different potentials were obtained with alternating current signals with amplitudes of 5 mV in the frequency range from 100 kHz to 10 mHz.

2.3. Composition identification and morphology characterization

Phase identification was carried out by X-ray diffraction (XRD) on a PAN analytical X'Pet-Pro-MPD (PW3050/60) instrument. A Leica metallographic microscope was employed to investigate the microstructure after etching by solutions composed of HNO_3: HF: H_2O=1:1:1. The compositions of the passivation films formed after potentiostatic polarization were identified by X-ray photoelectron spectroscopy (XPS) performed with a ESCALAB250 multifunctional surface analysis system (Thermo VG, America) using Al Kα radiation (1486.6 eV) at a pass energy of 50 eV and resolution of 0.1 eV. The observed binding energies (of Ti 2p, Si 2p, C 1s, O 1s and Al 2p) were referenced to the carbon C 1s peak at 284.6 eV. A Zeiss scanning electron microscope (SEM) coupled with an energy dispersive spectrometer (EDS) was used for analyzing the sample surface after corrosion.

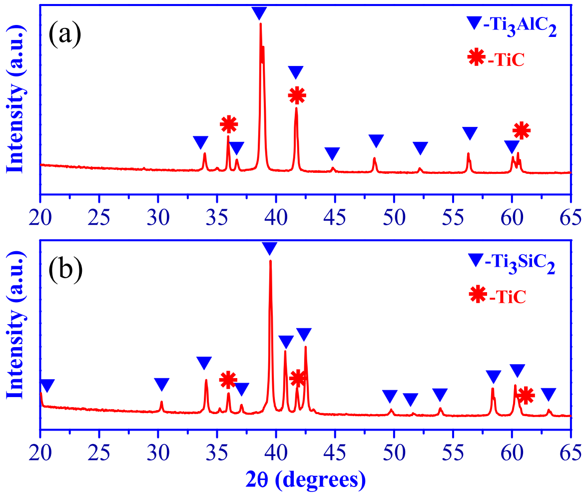

Fig. 1. XRD patterns of materials synthesized by in-situ solid-liquid reaction/hot pressing process for (a) Ti_3AlC_2 and (b) Ti_3SiC_2.

3. Results and discussion

3.1. Phase composition and microstructure

The X-ray diffraction patterns of Ti_3SiC_2 and Ti_3AlC_2 are shown in Fig. 1. The crystalline matrix phases were identified as Ti_3AlC_2 (Fig. 1a) and Ti_3SiC_2 (Fig. 1b). Peaks from an impurity phase (TiC) were detected by XRD in both coupons. The TiC contents in both matrices were calculated by quantitative phase analysis to be about 5% by volume. The samples prepared by this process had 98–99% of the theoretical density.

3.2. Potentiodynamic polarization and EIS measurement

Fig. 2 shows the potentiodynamic polarization curves collected from Ti_3SiC_2 and Ti_3AlC_2 in a 3.5% NaCl solution after 30 min of immersion. The anodic part of the polarization curves reveals an inflexion before 0.75 V followed by a decline. Both Ti_3SiC_2 and Ti_3AlC_2 exhibited passivation characteristics under anodic polarization. The peak at 0.75 V indicated that the corrosion and/or passivation mechanisms changed with increasing potentials. Electrochemical parameters such as self-corrosion potential (E_{corr}), self-corrosion current density (i_{corr}), passivation current density (i_p) and breakdown potential (E_b) were derived from the polarization curves (Table 1). Ti_3AlC_2 showed a poorer corrosion resistance at each measured voltage. In contrast to metals and alloys such as steel and chromium stainless

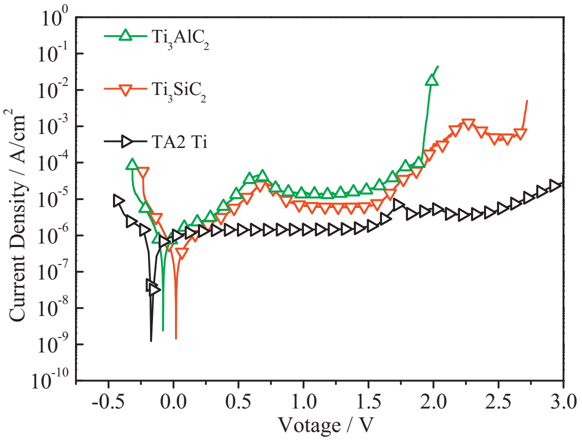

Fig. 2. Potentiodynamic polarization curves of Ti_3SiC_2, Ti_3AlC_2 and commercially pure Ti (CP Ti) in a 3.5% NaCl solution at scanning rate of 333μA/s.